DEVELOPMENT OF ANODIC ALUMINUM OXIDE TEMPLATES FOR GROWTH OF CuO NANORODS FOR PHOTODETECTION DIVICE

KHALED MAJID CHAHROUR

UNIVERSITI SAINS MALAYSIA

2016

DEVELOPMENT OF ANODIC ALUMINUM OXIDE TEMPLATES FOR GROWTH OF CuO NANORODS FOR PHOTODETECTION DEVICE

by

KHALED MAJID CHAHROUR

Thesis submitted in fulfillment of the requirements
for the degree of
Doctor of Philosophy

September 2016

ACKNOWLEDGEMENT

On this memorable day in my life, I reached the final destination of my PhD research study; first of all I bestowed the thanks to Allah Almighty for granting me health and patience with capability to complete this research work. I dedicate this thesis to the soul of my father, God have mercy on him. My heartfelt gratitude goes to all my family members for their continuous prayers, their support, and their encouragement. Words cannot sufficiently express how grateful I feel.

I would like to express my sincere thanks to my supervisor Dr. Naser Mahmoud Ahmed for his kind cooperation, useful contribution, and valuable guidance during my study and research work. I also wish to record my deep sense of gratitude to my co-supervisor Prof. Dr. Md Roslan Hashim for his useful and valuable suggestions, inspiring guidance, and consistent encouragement. He always taught me how to face hard moments in this research.

I acknowledge the Universiti Sains Malaysia (USM) Fellowship program for its financial support to this research. I express my gratitude as well to all staff members of the School of Physics, USM for their encouragement. To be fair I had to extend my sincere thanks to all of NOR laboratory staff for the cooperation and kindness behaviors with the all postgraduate students. I also thank all my friends and colleagues who supported me and helped me during the completion this thesis.

TABLE OF CONTENTS

LIST OF TABLES

LIST OF FIGURES

LIST OF ABBREVIATIONS

a.u	Arbitrary unit
AAO	Anodic aluminum oxide
Ae^-	Auger electrons
AFM	Atomic force microscope
Al	Aluminum
ALD	Atomic layer deposition
BSe^-	Backscattering electrons
CCD	Charge coupled device
CE	Counter electrode
CNT	Carbon nanotubes
CuO	Cupric oxide
CV	Cyclic voltammetry
CVD	Chemical vapor deposition
DC	Direct current
DI	Deionized water
E- beam	Electron beam
EDX	Energy dispersive X-ray spectroscopy
FESEM	Field emission scanning electron microscopy
IR	Infrared
I-t	Current-time
ITO	Indium tin oxide
I-V	Current-voltage
LV	Linear voltammetry

MBE	Molecular beam epitaxial
MS	Metal-Semiconductor
MSM	Metal-Semiconductor-Metal
NBE	Near-band edge emission
NRs	Nanorods
NTs	Nanotubes
NWs	Nanowires
pH	Power of hydrogen
PD	Photodetector
PL	Photoluminescence
PLD	Pulsed laser deposition
RCA	Radio Corporation of America
RE	Reference electrode
RF	Radio frequency
RIE	Reactive ion etching
RMS	Root mean square
Se^-	Secondary electrons
SPM	Scanning probe microscope
UV-VIS-NIR	Ultraviolet-Visible-Near infrared
WE	Working electrode
XRD	X-ray diffractometer

LIST OF SYMBOLS

A	Active area
c	Speed of light in vacuum
D_i	Interpore distance
D_p	Pore diameter
E	Irradiance of the light
E_C	Conduction band
$E_{exc.}$	Excitation energy
E_F	Fermi level of semiconductor
E_g	Semiconductor band gap
E_V	Valance band
h	Plank's constant
h, k, l	Miller indices
I_d	Dark current
I_{ph}	Photocurrent
k_p, k_i	Proportionality constants
n	Order of reflection
^oC	Celsius temperature
P	Porosity
P_{inc}	Incident optical power
q	Electron charge
R	Responsivity
R_p	Growth rate of AAO film

S	Sensitivity
V	Voltage
V	Volume
W	Pore wall thickness
β	Barrier layer thickness
η	Quantum efficiency
θ	Incident/Diffraction angle
λ	Wavelength
ν	Frequency of light
ρ	Pore density
φ_B	Schottky barrier height
φ_m	Metal work function
φ_s	Semiconductor work function
χ	Semiconductor electron affinity
$\check{\xi}$	Volume expansion
a, b, c, β	Lattice parameters

PEMBANGUNAN ACUAN ANOD ALUMINUM OKSIDA UNTUK PENUMBUHAN ROD NANO CuO DALAM PENGESANAN FOTO

ABSTRAK

Nanoliang anod aluminium oksida (AAO) bertertib tinggi dan berbentuk heksagon berjaya ditumbuhkan daripada saput prapemendapan Al dengan ketebalan 1μm pada substrat Si dan ITO/kaca melalui penganodan dua-langkah. Mekanisme pertumbuhan saput liang AAO dikaji berdasarkan penganodan perlakuan arus-masa pada voltan yang berbeza, dan juga melalui pemerhatian mikrostruktur menggunakan keratan rentas dan pandangan atas daripada pengimejan (FESEM). Kajian mendapati liang dengan diameter (garis pusat) yang berjulat daripada 50 hingga 110 nm dan ketebalan di antara 250 dan 1400 nm, diperolehi dengan mengawal pengaruh dua parameter utama penganodan, iaitu voltan penganodan dan masa penganodan langkah kedua. Keadaan optimum pemboleh ubah proses seperti masa penyepuhlindapan bagi saput nipis Al yang termendak dan masa pelebaran liang daripada saput liang AAO ditentukan secara eksperimen bagi memperoleh saput AAO dengan mikrostruktur liang yang teragih secara seragam dan yang dijajar secara menegak. Pelebaran liang melalui rawatan punaran basar pada suhu bilik didapati mengubah kualiti liang saput AAO dan mengurangkan saput halangan bawah jajaran liang untuk memudahkan elektroenapan struktur nano ke atas saput AAO. Sebagai tambahan, permukaan Al yang cekung hemisfera memastikan bahawa pentertiban atau penyusunan kendiri liang AAO boleh diwujudkan apabila penjaluran digunakan selama 45 minit. Justeru, dapat dirumuskan bahawa tempoh rawatan punaran basar (penjaluran) pada saput Al oksida berlaku selepas

penganodan langkah pertama memainkan peranan penting dalam susunan terakhir nanoliang. Analisis belauan sinar-X menunjukkan transformasi fasa amorfus - kepada - hablur selepas penyepuhlindapan pada suhu melebihi 800^{o}C. Imej AFM menunjukkan susunan optimum saput liang AAO teranod di bawah keadaan voltan yang rendah. Saput AAO boleh berfungsi sebagai templat dengan taburan saiz yang dikehendaki bagi fabrikasi jajaran nanorod CuO. Keputusan menunjukkan bahawa morfologi jajaran nanorod CuO yang dijajar amat terkesan oleh tempoh punaran basar dan penanggalan templat AAO. Kajian ini juga menunjukkan bahawa tempoh punaran basar optimum diperlukan untuk mengekalkan nanorod CuO dijajar tanpa sebarang fraktur adalah hampir 5 minit. Jajaran nanorod CuO prestasi tinggi /himpunan AAO dan pengesan foto IR susunan jajaran nanorod CuO yang berdiri bebas berdasarkan MSM difabrikasi dengan elektrod sentuhan-Al. Sambutan fotoelektrik dan elektrik dikaji, dan keputusan menunjukkan bahawa pengesan foto mempamerkan kepekaan yang tinggi terhadap diod laser infra merah (IR) 808 nm. Kedua-dua sambutan dan masa pemulihan didapati lebih cepat, iaitu masa yang lebih pendek dibandingkan dengan pengesan foto IR lain, yang dilaporkan dalam literatur.

DEVELOPMENT OF ANODIC ALUMINUM OXIDE TEMPLATES FOR GROWTH OF CuO NANORODS FOR PHOTODETECTION DEVICE

ABSTRACT

Ordered and hexagonal-shaped nanoporous anodic aluminum oxide (AAO) was successfully grown from 1μm thickness of Al pre-deposited onto Si and ITO/glass substrate using two-step anodization. The growth mechanism of the porous AAO film was investigated by anodization current-time behavior for different anodizing voltages and by microstructural observations using cross-sectional and top view of FESEM imaging. It was found that pores with diameter ranging from 50 to 110 nm and thicknesses between 250 and 1400 nm, were obtained by controlling two main influential anodization parameters: the anodizing voltage and time of the second-step anodization. The optimum conditions of the process variables such as annealing time of the as- deposited Al thin film and pore widening time of porous AAO film were experimentally determined to obtain AAO films with uniformly distributed and vertically aligned porous microstructure. Pore widening via wet-etching treatment at room temperature was found to modify the pore quality of AAO films and reduces the barrier layer on the bottom of AAO pore array facilitating a uniform electrodeposition of nanostructures onto AAO films. In addition, regular hemispherical concave Al surface ensuring the self-ordering of AAO pore can be established when striping is employed for 45 min. Thus, it could be inferred that the duration of wet etching treatment (striping) of Al oxide film performed after the first-step anodization plays a crucial role in the final arrangement of nanopores. X-ray diffraction analysis revealed amorphous-to-crystalline phase

transformation after annealing at temperatures above 800 ^{o}C. AFM images showed optimum ordering of the porous AAO films anodized under low voltage condition. AAO films could serve as templates with desired size distribution for the fabrication of CuO nanorod arrays. The results indicated that the morphology of the aligned arrays of CuO nanorods was strongly affected by the duration of etching and the removal of AAO template. This study showed also that the optimum etching duration required to maintain the aligned CuO nanorods without any fracture was approximately 5 min. High performance CuO nanorod arrays/ AAO assembly and free-standing CuO nanorod arrays infrared (IR) metal-semiconductor-metal (MSM) photodetectors were fabricated with Al contact electrodes. The electrical performance and photoelectric response were studied and the results showed that IR photodetectors exhibited a high sensitivity to 808 nm IR laser diode. Both the response and recovery time were found to be fast; i.e. much shorter time compared to other IR photodetectors reported in the literature.

CHAPTER 1

INTRODUCTION

1.1 Introduction

Nanotechnology "the science that deals with nanometer-sized structures" is a fast-growing interdisciplinary field that extends exciting research in many fields, including physics, chemistry, material science and biology. Nanostructures exhibit unique physical and chemical properties due to quantum confinement effect compare to bulk counterparts. In recent years, many efforts have been focused on the development of expensive and inexpensive nanofabrication techniques. The large scale inexpensive fabrication methods remain one of the key mainstays of today's nanotechnology. The search for such in low-cost fabrication alternatives, reaching the limits of current technologies, has led to a growing interest in nanoporous materials as templates for the controlled growth of nanostructures.

In particular, the porous anodic aluminum oxide (AAO) films formed by the electrochemical anodizing of aluminum have received significant attention in the synthetic nanostructure materials. The successful application of porous AAO as templates in many industrial fields, such as the manufacturing of nano-optoelectronic devices, is attributed to their highly controllable pore diameter and cylindrical shape, as well as periodicity and density distribution. In addition, AAO is electrically insulating, transparent and possessed high chemical and heat stabilities.

Previous studies have deduced that the most significant controllable parameters that influence the preparation of porous AAO films are the anodizing

voltage, type/concentration of the electrolyte, temperature and duration of anodization. For instance, by the controlling of the voltage during anodization, the possibility of modifying pore diameter as well as interpore distance increases exponentially. The thickness of the AAO films can also be modified by controlling the duration of anodization process.

Masuda and Fukuda [1] and Jessensky *et al.* [2] were the pioneers in describing how to fabricate an AAO template onto bulk Al foil with ordered hexagonal-shaped parallel nanotubes using a two-step anodization process. It has been reported that in order to obtain fully ordered nanotubes throughout the template, it is necessary to introduce a pre-arranged pattern before anodization. It was suggested that the anodization should be carried out in two steps. Most of the developed methods for producing self-organized AAO templates generally yield highly ordered arrays onto bulk Al foil. However, some challenges were encountered during the preparation of porous AAO templates of Al pre-deposited onto conducted substrates by using two-step anodization, including achieving highly-ordered porous AAO with open-through bottom barrier layer of pore structure.

In literature, different approaches have been used in the preparation of nanostructures into porous AAO template, such as chemical vapor deposition (CVD), physical vapor deposition (PVD) and electrochemical deposition. In the current research, the preparation of metallic nanostructures such as copper into porous AAO using electrochemical deposition, followed by thermal oxidation is the most promising and efficient method for the growth of vertically aligned cupric oxide nanorod arrays. The cupric oxide (CuO) has been a hot topic among the studies on transition metal oxides, because of its interesting properties as a p-type

semiconductor with a narrow band gap. The vertically aligned CuO nanorod arrays with large surface areas and size potential effect possesses superior physical and chemical properties. These significant CuO nanostructures have been extensively investigated, because of their promising applications in the photodetection devices.

1.2 Problem Statement

During the two-step anodizing of Al thin film deposited onto substrate, due to the limited thickness of Al (≤ 1 μm), the fabrication of uniform porous structure with vertically aligned nanotubes are not easily applicable. Also in the case of long time anodizing, which is known for producing well-ordered pore structure, the Al thin film can be easily detached from the substrate or develop cracks. These problems make the identification of optimum conditions to attain the required pore size, pore density and pore uniformity much more complex to be achieved in this research. Inability in optimizing the duration of pore widening prevents attaining high quality features of AAO pore arrays and obtaining homogeneous electrodeposition of nanostructures into AAO template. Nanorods fabricated using AAO are characterized by highly ordered and vertically well aligned nanostructures. However, the removal of AAO template causes the nanorods to collapse easily or aggregate into clusters due to their high surface tension. This has a negative influence on the fabrication of photodetection devices. Consequently, the control of the wet etching treatment procedure for the removal of AAO template has become imperative.

1.3 Research Objectives

The main objectives of this research work can be summarized by the following points:

1. To synthesize highly-ordered thin AAO template onto Si and ITO/glass substrate, and study their growth parameters by controlling the intrinsic variables of anodization, including anodizing voltage and duration of the second-step anodization.
2. To develop a simple and efficient method to prepare uniform CuO nanorod arrays embedded into Si-based AAO template.
3. To study characteristics and performance of IR photodetectors based on aligned CuO nanorod arrays grown on Si substrate with or without AAO template.

1.4 Research Originality

The originality of this research work can be identified as follow:

1. Controllable pore-widening process by adjusting the pore diameter and removing the AAO bottom barrier layer at room temperature.
2. Microstructural procedure of the thin AAO film fabrication via two-step anodization has been visualized for the first time by using a cross-sectional FESEM imaging.
3. Elucidate a possible relationship between the morphology of aligned arrays of CuO nanorods during removal of AAO template and etching time, which has been reported for the first time.
4. No previous reports can be found in the literature so far about the fabrication of aligned CuO nanorod arrays IR metal-semiconductor-metal (MSM) photodetector by assisted AAO template.

5. Fabrication Al-CuO nanorod arrays-Al IR photodetector with ultra-fast response and recovery times at zero bias voltage.

1.5 Thesis Overview

The content of this thesis is organized as follows: Chapter one contains a brief overview of an inexpensive and successful fabrication of the nanostructures by using self-organized porous AAO template, the main research problem, the research objectives and research originality. Chapter two presents a literature review and theoretical background of this study. Chapter three describes the principles of the experimental equipment, fabrication process and characterization instruments used in the preparation of porous AAO templates, growth of CuO nanorod arrays and for photodetection device applications. In chapter four, thin porous AAO films under controllable conditions of two-step anodization grown from pre-deposited Al thin film (1μm) thick onto Si and ITO/glass substrate are fabricated. The modulation of the AAO features (pore diameter and pore length) by modifying two controllable conditions (anodizing voltage and time of anodization) is involved in this chapter. In addition, this chapter explains the effect of the chemical wet etching time cycles (striping of the first-step anodization and pore widening) on the morphological features of Si-based AAO templates. The growth and characterization of CuO nanorod arrays into thin porous AAO template, as well as, fabrication and characterization of two MSM photodetector devices: Al-CuO nanorod arrays/AAO assembly-Al and Al-CuO nanorod arrays-Al are investigated in chapter five. Finally, conclusions and recommendations for future studies are reported in chapter six.

CHAPTER 2

LITERATURE REVIEW AND THEORETICAL BACKGROUND

2.1 Introduction

In this chapter, general fundamentals and basic theories of all required subjects involved in this research study are presented. It begins with classification of the AAO films into two categories according to their morphology. The advantage of heat treatment on Al films before anodization is clarified briefly. The mechanism of pore nucleation of the AAO is discussed. The procedure of self-organized of porous AAO by using two-step anodization is explained. The effect of anodizing parameters on modulation of the pore dimensions is reviewed. The growth of nanostructure materials by electrodeposition assisted porous AAO film also is reviewed. Moreover, the essentials of metal–semiconductor contacts and the basic principles of the metal-semiconductor-metal photodetectors are briefly described in this chapter.

2.2 Types of Anodic Aluminum Oxide (AAO)

Anodization of Al films in aqueous electrolytes produces anodic oxide films with two different morphologies, that is, the nonporous barrier-type oxide films and the porous-type oxide films. The different morphology depends on the chemical nature of the electrolyte [3-5].

2.2.1 Nonporous Barrier-Type Oxide

Barrier-type films are generally grown in an electrolytic cell with neutral electrolytes such as borate, oxalate, citrate, phosphate solution, etc. The grown film is insoluble in the electrolyte and consists of a thin compact layer of aluminum oxide

[6, 7]. Barrier-type oxide formation under potentiostatic conditions, current density (j) decreases exponentially with time (t). Correspondingly, the film growth rate decreases almost exponentially with time (t), which points a limit on the maximum film thickness obtainable for barrier-type AAO films (Figure 2.1 (a)). It has been experimentally verified that the thickness of barrier-type film is directly proportional to the applied voltage.

2.2.2 Porous-Type Oxide

Porous-type films are generally grown in an electrolytic cell with acidic electrolytes such as sulfuric [8], oxalic [9], phosphoric [10], chromic [11], malonic [12], tartaric [13], citric [14], squaric [15], malic acid [16] etc., in which anodic oxide is slightly soluble and consist of arrays of cylindrical shaped pores surrounded by an aluminum oxide structure.

Current density (j) in porous-type anodization under potentiostatic conditions remains almost constant within a certain range of values during the anodization process, due to the constant thickness of the barrier layer at the pore bottom (Figure 2.1 (b)). The thickness of the resulting porous oxide film is linearly proportional to the total amount of charge (i.e., anodization time) involved in the electrochemical reaction. It has been experimentally verified that the thickness of porous-type film is directly proportional to the anodization time.

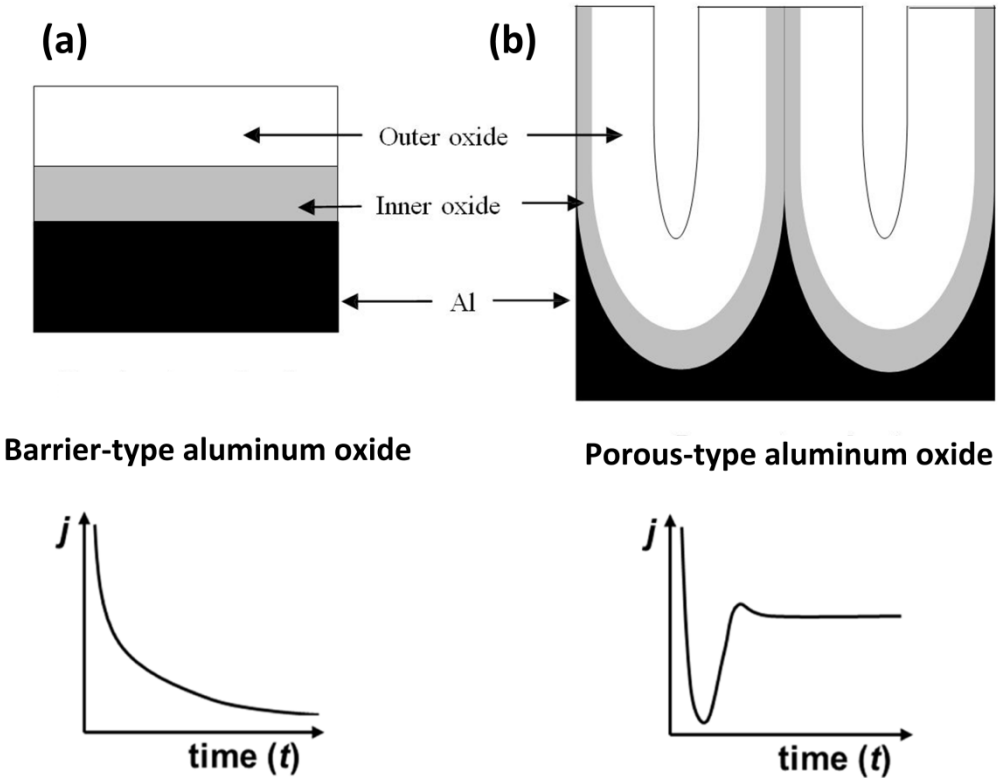

Figure 2.1 Two different types of anodic aluminum oxide (AAO) formed by (a) barrier-type and (b) porous-type anodizing process, along with the respective current density - time (j-t) transients under potentiostatic conditions [17].

2.3 Pre-Treatment of Al Films

The quality of the surface structure and/or the surface pre-treatments of the Al film will have a significant impact on the morphology and the nanoporous structures formed on the film surface during the anodizing process [18-21]. The purity of the Al film used has a direct impact on its dissolution rate in the acidic conditions of the electrolyte and thus, high purity Al is generally used. A purity of 99.99 % is commonly used. A typical pre-treatment of an Al film begins by first, degreasing the Al film using acetone or a similar solvent, then electrochemically polished in 1 M of sodium hydroxide solution for few minutes and finally washed in deionized water. This is followed by the annealing treatment; which is applied to the Al film to reduce

the mechanical stresses in the material and to modify the grain boundaries, since both these factors can have a significant effect on pore nucleation [22]. Annealing is usually performed at a temperature close to two-thirds of the melting point of Al usually between (400 - 500 °C) in an inert atmosphere, such as nitrogen or argon inside a conventional furnace [23]. The Al film is kept at this temperature for a suitable annealing period usually between (2 - 5 h) and then allowed to slowly cool in the inert atmosphere to prevent oxidation. During the annealing process the Al crystals reoriented to a preferred crystalline direction [24] and the Al grain size increases and the surface of the Al film becomes rougher and the larger grain boundaries can be observed [25, 26].

2.4 Mechanism of Pore Nucleation

The origin of pore nuclei and the exact mechanism of pore nucleation are still clearly unknown. Several formation models have been proposed; one model explains that pore nucleation result from an electric field-assisted dissolution theory was first proposed by Hoar and Mott [27], but its effect on pore size, spacing and other porous AAO features were only presented in detail a few years later [28]. Thompson and Wood pioneered the understanding on the morphology, ion transport and initial stages of pore formation in porous AAO [29]. This model explains that pore nucleation results from an electric field assisted dissolution at the electrolyte/oxide interface and oxide generation at the metal/oxide interface.

In the early stages of the anodizing process, Al^{3+} ions migrate from the metal across the metal/oxide interface into the forming oxide layer. In the same time O^{2-} ions formed from water at the oxide/electrolyte interface travel into the oxide layer [30, 31]. During the oxide formation the barrier layer constantly regrows with further

oxide growth and transforms into a semi-spherical oxide layer of constant thickness that forms the pore bottom, as shown in Figure 2.2. During the formation of the porous oxide layer the anodic Al dissolution reaction is presented by

$$2Al \rightarrow 2\,Al^{+3} + 6e^{-} \quad (2.1)$$

The resulting reaction at the cathode produces bubbles of hydrogen gas:

$$6H^{+} + 6e^{-} \rightarrow 3H_2 \quad (2.2)$$

Anode reactions taking place at the metal/oxide interface (Oxygen anions react with Al)

$$2Al + 3O_2^{-} \rightarrow Al_2O_3 + 6e^{-} \quad (2.3)$$

At the oxide/electrolyte interface (Al cations react with the water molecules)

$$2Al_3^{+} + 3H_2O \rightarrow Al_2O_3 + 6H^{+} \quad (2.4)$$

Overall reactions at electrode describe the simple reaction of anodizing process.

$$2Al + 3H_2O \rightarrow Al_2O_3 + 3H_2 \quad (2.5)$$

The steady state growth results from the equilibrium between the field-assisted oxide dissolution at the oxide/electrolyte interface at the base of the hemispherical shaped pores where the electric field is high enough to drive the Al^{3+} ions through the barrier layer and the oxide growth at the metal/oxide interface resulting from the migration of O^{2-} and OH^{-} ions into the pore base oxide layer.

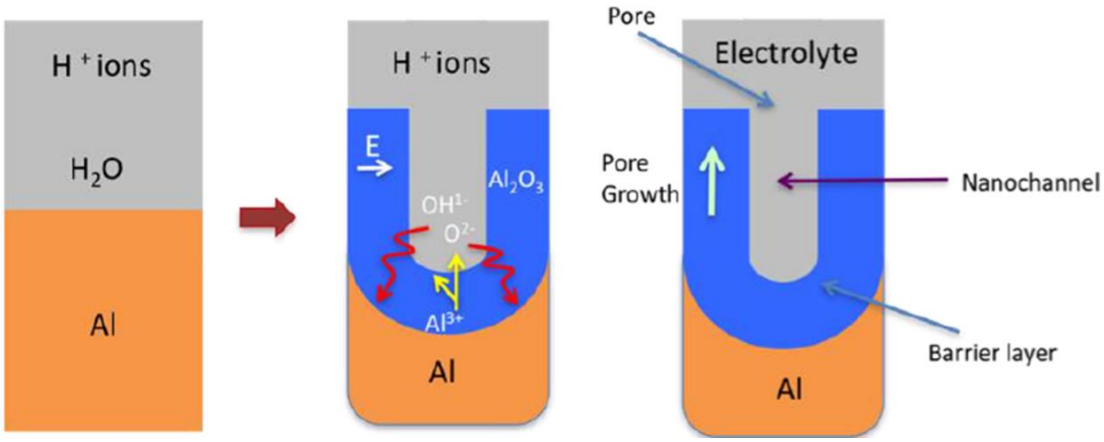

Figure 2.2 Schematic of the pore nucleation mechanism in an acidic electrolyte [32].

Shimizu *et al.* [33] described the initial pore formation process as a transition from a barrier-type film to a porous-type film, created by the cracking of the Al film under tensile stress, where the locally thinner sites become preferred sites for pore development. A theoretical model based on oxide growth at the metal/oxide and oxide/electrolyte interfaces and on field-assisted dissolution at the pore bottom, was then proposed by Parkhutik and Shershulsky [34]. Although a description of the porous AAO formation and growth was provided in this model.

Thamida and Chang [35] proposed a mathematical model accounted the effect of the surface curvature (roughness, perturbations) on converging the electric field at the troughs and diverging at the crests. Recently, a linear correlation between AAO pore depth and electric charge density during electrochemical anodizing process was determined and utilized to facilitate precise control of the porous AAO growth process in a wide range of voltage for a broad application [36].

In addition, the time dependence of the anodizing current during porous AAO formation is well established and can also provide insights into the growth process. Figure 2.3 shows a typical electric current curve monitored during the anodizing process where distinct regimes indicative of porous AAO structure formation can be identified [4, 25, 37, 38].

At first, the electric current decreases, it corresponding to the formation of barrier-type oxide film (regime (I)). Then, it passes through minimum value of electric current (regime (II)). Al is continuously oxidized and pore begin to grow in sites where irregularities on the surface topography. At these sites, the electric-field lines are converged, giving rise to localized heating due to electrical power dissipation. This effect results on enhanced chemical-assisted dissolution of the oxide. Subsequently, the electric current translates into a rise in value and it corresponds to the initial stage of pore nucleation and growth. In this stage numerous ionic conduction paths (pores) appear. Since some pores begin to stop growing due to competition among the pores, the current decreases again (regime (III)). Last, the electric current reaching a steady-state value (regime (IV)). The constant in electric current is indicative of equilibrium between oxide dissolution (at the electrolyte/oxide interface) and oxide growth (at the metal/oxide interface) giving a constant growth rate for the nanopores.

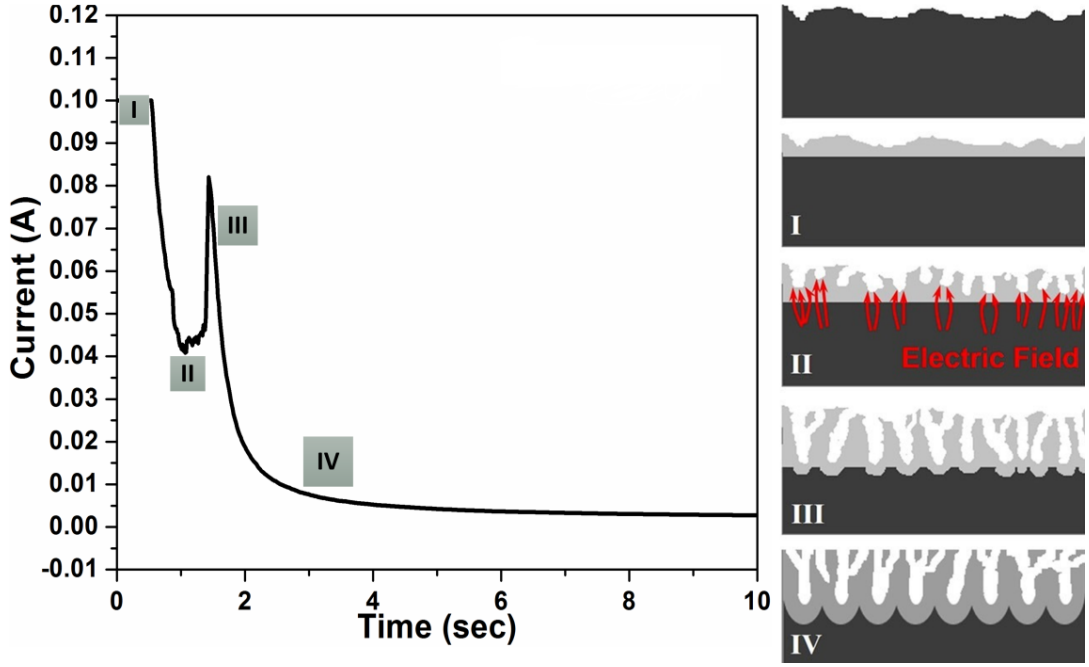

Figure 2.3 Current-time transients during porous AAO formation showing the distinct pore growth stages [39].

2.5 Self- Organized Porous AAO Film

Generally, there are two different techniques of porous AAO fabrication: a prepatterned-guided anodization resulting in a perfectly ordered nanopore arrangement and self-organized two-step anodization leading to a quasi-monodomain structure with partially areas of defects. The pre-patterning of Al film prior anodization can be carried out using a tip of the scanning probe microscope (SPM) [40, 41] and atomic force microscope (AFM) [42]. The patterning of Al film can be also formed by focused-ion beam lithography [43, 44]. Various molds with a regular array of convexes prepared lithographically have been also used for pre-patterning of Al film [45-47].

The main drawbacks of these pre-patterned anodization techniques are a time-consuming indentation of Al film before anodization and high-cost. Additionally, the perfect arrangement of nanopores of AAO is observed over the pre-patterned surface area of Al film only.

On the other hand, a self-organized two-step anodization of porous AAO can be carried out over a large surface area at the same time. The process of porous AAO formation by self-organized anodizing is simple, inexpensive and results in a high-density of nanopores but it is not free from defects in pore arrangement [37, 48, 49].

2.5.1 Two-Step Anodization

Masuda and Fukuda, 1995 developed a two-step anodization method to obtain highly ordered porous AAO, without resorting to complex and costly lithographic techniques [1]. Their procedure involved two separated anodization processes onto bulk Al foil: a longer first anodization until order at the metal/ oxide interface is attained followed by oxide removal and a subsequent second-step anodization (Figure 2.4). While the first-step anodization at the original pre-treatment Al surface, the pores nucleated in (almost) random positions (Figure 2.4 (c)), ordered domain of Al dimples with area larger than 1 μm are observed at the Al substrate top surface, after removing the porous aluminum oxide layer (Figure 2.4 (d)). During the second anodization, the pores will conveniently nucleate at the depressions of the Al surface, with the pattern guiding the nanopores growth. This leads to highly ordered hexagonal porous structures with domain of area larger than 1 μm, depending on the first anodization time (Figure 2.4 (e)).

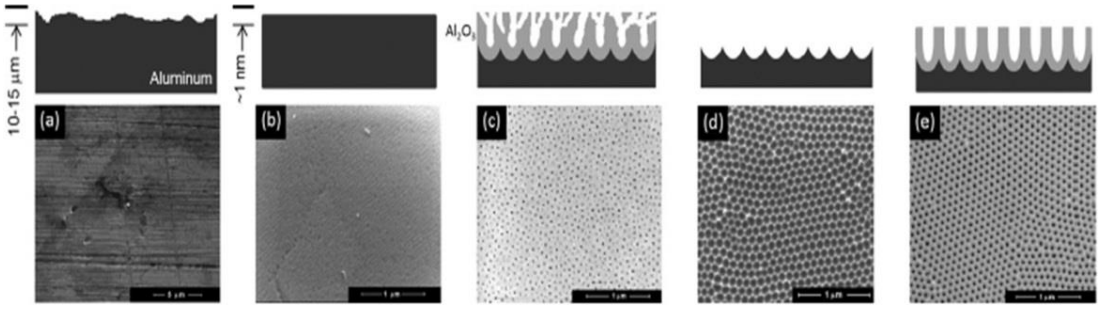

Figure 2.4 Two-step anodization method: schematic drawings and corresponding SEM images for anodization in 0.3 M oxalic acid, anodizing voltage is 40 V, temperature of electrolyte at 4 ^{o}C. (a) Al foil surface as-rolled; (b) Al foil surface after standard pre-treatments; (c) top porous-alumina surface with random pore nucleation; (d) Al substrate top surface after chemical etching of the aluminum oxide formed during the first-step anodization, evidencing the patterned dimples; (e) top porous AAO surface after a second-step anodization [39].

Many models pointed to slightly different mechanisms related to self-organized; one model explained the self-organized was a mechanical stress model proposed by Jessensky *et al.* [2, 50] based on repulsive forces between neighboring pores to explain the formation of hexagonally-ordered pore arrays. During the oxide growth at the metal/oxide interface, a volume expansion occurs (Figure 2.5) as a consequence of the lower atomic density that Al presents in Al_2O_3 when compared to metallic Al. While the oxide is growing, the significant volume (V) expansion ($\check{\beta}$ = $V_{Al_2O_3}/V_{Al}$) leads to mechanical stress in the barrier-layer, expansion pore walls to grow only on the vertical direction and pushes the pore walls upwards [51].

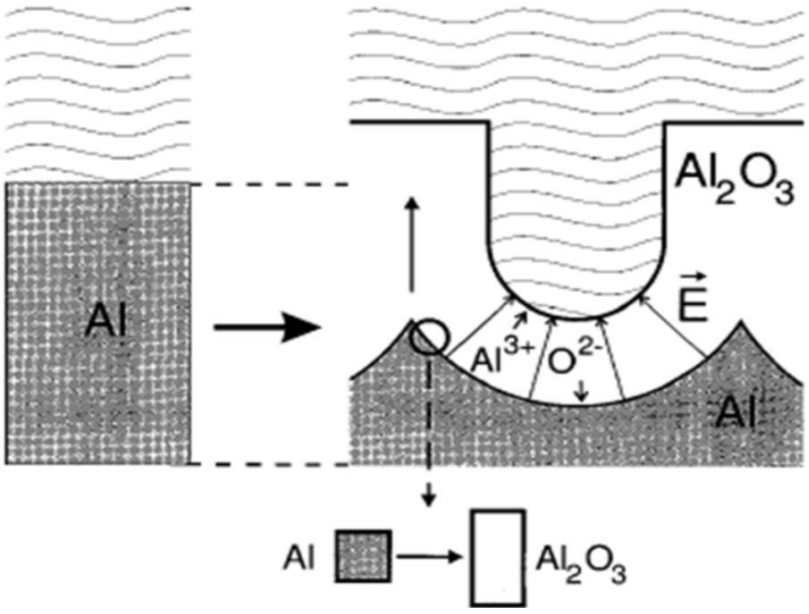

Figure 2.5 Expansion of Al during anodic oxidation, depicting on the left the level of the unoxidized metal surface [2].

However, not all oxidized Al gives rise to Al_2O_3, approximately 70% of the Al^{3+} ions and the O^{2-} ions contribute to the formation of the barrier oxide layer [30], the remaining Al^{3+} ions are dissolved into the electrolyte, and thus the real volume expansion was found to depend on anodizing voltage and electrolyte composition [52].

2.5.2 Structure Features of Self-Ordered Porous AAO Film

Figure 2.6 shows schematically an idealized structure of self-ordered porous AAO. Porous aluminum oxide layer formed on Al surface contains a large number of mutually parallel nanopores with honeycomb-like structure. Each circular nanopore consists of vertical pore channel and its surrounding aluminum oxide constitutes a hexagonal cell. The nanopore at the metal/oxide interface is closed by a thin barrier oxide layer with an approximately hemispherical morphology. The thickness of the

porous AAO layer on Al surface is easily tunable from a few tens of nanometers up to hundreds of micrometers by controlling the anodizing time [53].

In general, the structure of porous AAO is often defined by several structural features, such as interpore distance (D_i), pore diameter (D_p), barrier layer thickness (β), pore wall thickness (W), pore density (ρ), defined as number of pores on the surface area of 1 cm^2, and porosity (P), defined as a ratio of a surface area occupied by pores to the total surface area of oxide. Depending on experimental results, these structural features are mainly determined by anodizing parameters.

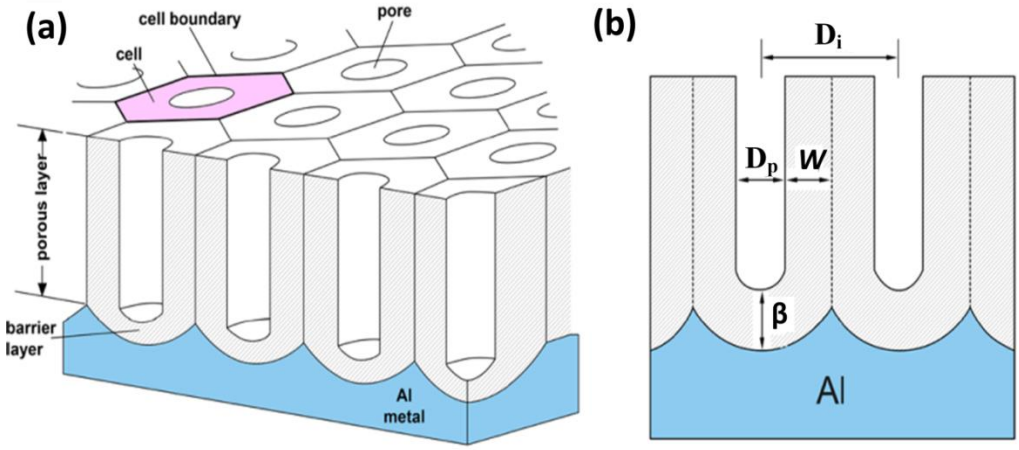

Figure 2.6 Schematic structure of (a) porous anodic aluminum oxide (AAO) on Al foil and (b) cross-sectional view [17].

For ideally ordered porous AAO, the different features can be calculated from the well-known Equations established for hexagonally arranged nanoporous structures [49]:

$$D_i = D_p + 2W \quad \text{(nm)} \tag{2.6}$$

Where, D_i is interpore distance, D_p is pore diameter and W is pore wall thickness.

$$\rho = \frac{2 \times 10^{14}}{\sqrt{3} \times D_i^2} \quad (cm^{-2}) \tag{2.7}$$

Where, ρ is the pore density and D_i is interpore distance.

$$p(\%) = \frac{\pi}{2\sqrt{3}} \times \left(\frac{D_p}{D_i}\right)^2 \tag{2.8}$$

Where, p is the porosity, D_p is pore diameter and D_i is interpore distance.

Highly-ordered hexagonal structures can be obtained of optimum parameters of anodizing process (Table 2.1), which samples exhibit a porosity *P* of ~ 10 %, and corresponding volume expansion $\breve{\jmath}$ = 1.2 [51]. In the case of sulfuric and phosphoric acid, the porosity for the optimum conditions is slightly higher than the expected 10 %, due to chemical etching of the aluminum oxide pore wall.

Table 2-1 Controllable parameters: anodizing voltage, concentration and temperature of the electrolyte and structural features: interpore distance (D_i), pore diameter (D_p), pore wall thickness (*W*), porosity and growth rate of self-organized porous AAO for sulfuric, oxalic and phosphoric acid [39].

Acid	**Sulfuric**	**Oxalic**	**Phosphoric**
Voltage (V)	25	40	195
Concentration (M)	0.3	0.3	0.1
D_i (nm)	65	105	480
D_p (nm)	25	35	180
W (nm)	~34	~50	~250
Porosity (%)	~14	~10	~13
Growth rate (μm/h)	5	2.5	5
Temperature (^oC)	~1	~4	~1

2.6 Modulation of the Pore Dimensions

The controllable fabrication of thin porous AAO template under parameters conditions of anodizing process by using two-step anodization with tailoring the pore diameter, interpore spacing, thickness of thin porous AAO template through controllable of the critical parameters of anodizing process such as, anodizing voltage, concentration and electrolyte type and temperature are well-known effects [54-59].

2.6.1 Anodizing Voltage

The anodizing voltage, V, is one of the most important factors to adjust self-organized of porous AAO film. As shown in the Figure 2.7, the interpore distance (D_i), is linearly proportional to the applied voltage with a proportionality constant k_i (nm/V) of approximately value is equal 2.5 for different types of acidic electrolyte [13, 52, 60].

$$D_i = k_i V = 2.5 V \quad (2.9)$$

In addition, large efforts have been made in the last years to widen the voltage vs. D_i range. Up-to-now, ordered porous AAO has been prepared in broad interval conditions as seen in the Figure 2.7 [39, 60, 61].

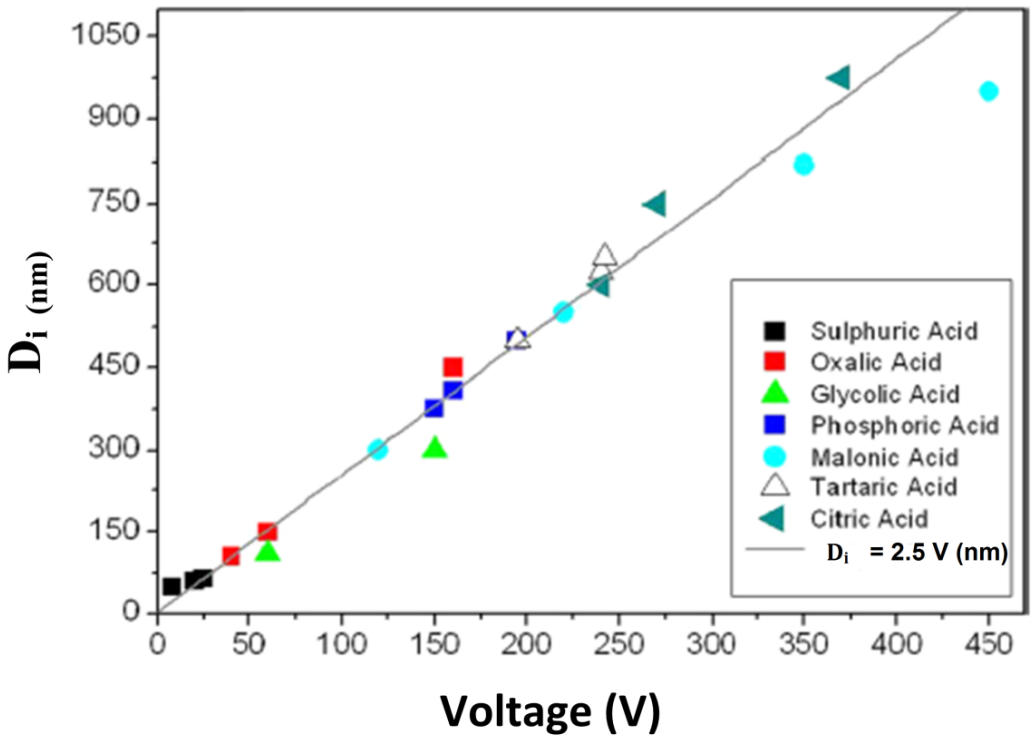

Figure 2.7 Interpore spacing versus anodizing voltage. The known self-ordering regimes are shown as symbols. The line is a fit to the data with a proportional constant k_i = 2.5 nm/V. Experimental data extracted from Chu *et al.* [13] and Ono *et al.* [60].

The model proposed by O'Sullivan *et al.* [28] showed a linear relation between the pore diameter (D_p) and the anodizing voltage. This relation was clarified by Xu *et al.* [62], which depends of the migration velocity of the reactive ions under the electric field during the growth and dissolution process of the forming porous AAO. This clarification was later supported by the study of Shingubara *et al.* [63] who investigated that voltage dependence on pore formation. A few years later, Lee *et al.* [64] reported that pore diameter (D_p) increases with current density (j) under potentiostatic anodization. Recently, many studies describe the fabrication of porous AAO with modulated of pore diameters by oscillatory current signals (anodization cyclic) [65].

Two other features (pore density and porosity) that characterize the porous AAO are related with the anodizing voltage. The pore density varies inversely as the square of the anodizing voltage [66]. Using 3 % oxalic acid, pore densities of the order 10^{10} pores/cm^2 can be obtained. Pore densities (>10^{11} pores/cm^2) can be obtained using 15 % sulphuric acid. Exponential dependence of pore density as a function of anodizing voltage was reported by Palibroda *et al.* [67]. In order to obtain perfect self-organized hexagonal arrays of nanopore formed during optimal anodizing parameters, the porosity of 10 % rule should be obeyed [51]. Recently, reports have published regarding changes in the porosity of porous AAO with increasing anodizing voltage [68, 69].

2.6.2 Type and Concentration of the Electrolyte

The type and concentration of the electrolyte for a given anodizing voltage has to be selected properly to obtain self-ordered pore growth. In other words, the choice of the type of electrolyte is limited. Usually, the anodization of Al is carried out in sulfuric acid in low voltage range 5- 25 V, oxalic acid is used for medium voltage range 35- 80 V and phosphoric acid for high voltage range 80- 200 V. This limit is due to the conductivity and pH value of the electrolyte. For example, if Al is anodized in sulfuric acid at a high voltage (note that sulfuric acid has a very high conductivity), collapse of the porous AAO layer takes place very often. In addition, the pH-scale of the electrolyte determines the diameter of the pores. The lower the pH scale, the lower the voltage threshold for field-assisted dissolution at the pore boundary. This leads to a smaller size of the pores. Therefore, small pore diameters are formed by using the sulfuric acid, the medium pore diameters are formed by using the oxalic acid and the large pore diameters are obtained by using the

phosphoric acid [25]. Theoretical modeling of porous AAO growth performed by Parkutik and Shershulsky [34] predicted an increase in pore diameter with increasing pH electrolyte. (i.e., increasing electrolyte concentration) due to the enhanced dissolution velocity of anodic oxide at the pore base. Nielsch *et al*. [51] proposed the 10% porosity rule for the self-ordering regimes in three electrolytes such as sulfuric, oxalic, and phosphoric at anodizing voltages 25, 40, and 195 V, respectively as shown in Figure 2.8.

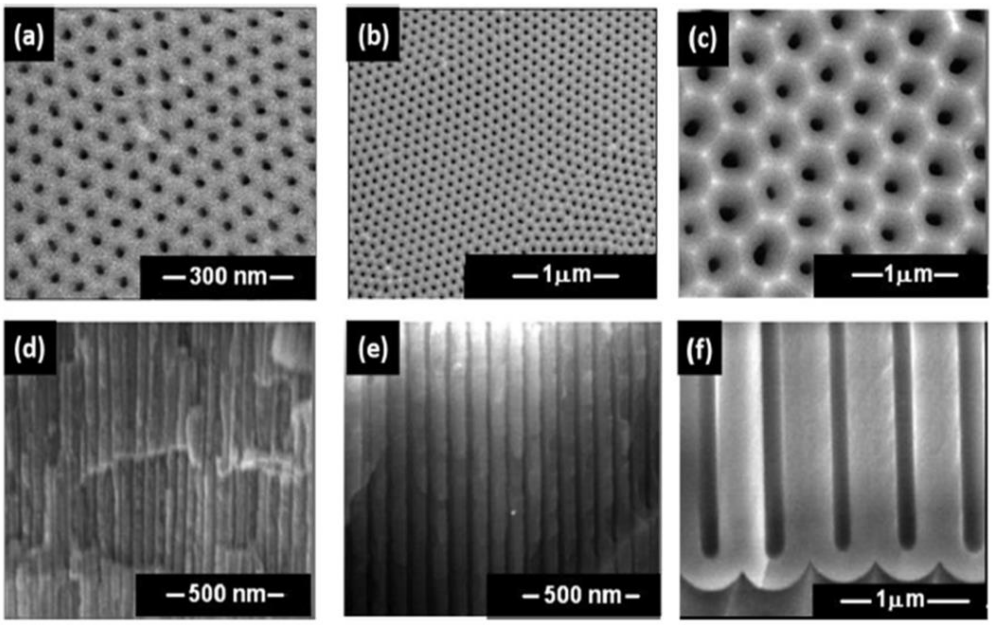

Figure 2.8 (a, b and c) Top surface and (d, e and f) cross-section SEM image of porous AAO obtained with different anodizing parameters: [(a) and (d)] 0.3 M sulfuric acid, anodizing voltage is 25 V; [(b) and (e)] 0.3 M oxalic acid, anodizing voltage is 40 V; [(c) and (f)] 0.1 M phosphoric acid, anodizing voltage is 195 V [39].

2.6.3 Temperature Dependence

During the anodizing process, temperature should be kept lower than room temperature to prevent the formed oxide structure from being dissolved in acidic

electrolytes. For instant, anodization at 40 V in oxalic acid is performed at 5- 19 ^{o}C and in the case of anodization at 195 V in phosphoric acid is performed at 0- 2 ^{o}C. Additional reason to keep the temperature as low as possible is to avoid a local heating at the bottom of the pores during the period of anodization (specially, the anodizing process at a high voltage). The local heat causes an inhomogeneous electric field distribution at the bottom, leading to local electrical collapse of the oxide layer. Recently study by Sulka and Parkoła indicated that the pore diameter increases with increasing temperature [58]. During the anodizing process, the electrolyte should be vigorously stirred to efficiently remove local heat and hydrogen bubbles on the Al surface, and to allow a homogenous diffusion of anions into pore channels [70].

2.7 Syntheses of Functional Nanostructures Assisted by Porous AAO

Synthesis of functional nanostructures into porous AAO template provides many unique opportunities, allowing simple and cost-effective preparations of extended high-ordered arrays of nanostructures and also overcoming many of drawbacks of conventional state of the art lithographic techniques.

2.7.1 Porous AAO Deposited onto Substrates

There are two major kinds of porous AAO, the first- type of porous AAO is grown on a bulk pure Al foil while the second- type is grown on conductive or metal-coated substrates. The second- type of the porous AAO is preferable. In addition to overcoming the brittle characteristics of porous AAO originated from Al bulk after removal the Al backing, porous AAO grown onto thin Al film (> 1 μm) deposited on conductive or metal-coated substrates would potentially offer much broader

application than those on bulk Al foils [71, 72]. The substrate could be semiconductor such as Si [73-78], non-valve metal (e.g., Cu, Ag, Au, Pt, etc.)-coated Si substrates [72, 79-82], valve-metal (e.g., Ti, W, Ta, etc.)-coated Si substrates [83-85] and transparent indium tin oxide (ITO) [86-89].

Most of the developed methods for producing porous AAO generally yield highly ordered arrays on bulk Al foil. Until now, the fabrication of highly ordered thin porous AAO on substrates is difficult to be formed mainly due to the complicated surface states (roughness and crystallite sizes) and non- uniformity of the deposited Al film [71, 87] and still remains a major challenge from the scientific and technological point of view [90]. Moreover, the degree of pore ordering remains relatively not highly, even if a two-step anodization process is used, because of the limited thickness ($\leq$ 1 μm) of the Al film [88].

Porous AAO formed by anodizing thin Al films on substrates have been successfully utilized not only as patterning masks, but also as templates for fabricating various functional nanostructures (nanotubes, nanorods, nanowires and nanodots), including ordered arrays of metal [71, 91-93], semiconductor [84, 94-96], carbon nanotubes (CNT) [97-99], or polymer [100, 101] on various substrates.

2.7.2 Removing Bottom Barrier Layer

Despite the broad range of potential applications of Si- based or ITO/glass-based AAO film, the prevalent problem is the barrier layer formed at the bottom of the AAO pores, which inhibits direct physical and electrical interaction with the substrate. Hence, diverse techniques have been employed to remove the bottom barrier layer such as, pore widening [72, 102], cathodic polarization [74, 103], voltage drop [104, 105] and reactive ion etching (RIE) [106, 107].